Research Journal of Applied Sciences, Engineering and Technology 7(20): 4303-4312, 2014
DOI:10.19026/rjaset.7.802
ISSN: 2040-7459; e-ISSN: 2040-7467

Submitted: December 28, 2013 Accepted: January 16, 2014 Published: May 20, 2014

Research Article

Sensor-less Field Oriented Control of Wind Turbine Driven Permanent Magnet Synchronous Generator Using Flux Linkage and Back EMF Estimation Methods

[1]Porselvi Thayumanavan, [2]Ranganath Muthu and [3]Jeyasudha Sankararaman
[1]Department of EEE, Sri SaiRam Engineering College, Chennai, India
[2]Department of EEE, SSN College of Engineering, Chennai, India
[3]Department of EEE, Sri SaiRam Engineering College, India

Abstract: The study aims at the speed control of the wind turbine driven Permanent Magnet Synchronous Generator (PMSG) by sensor-less Field Oriented Control (FOC) method. Two methods of sensor-less FOC are proposed to control the speed and torque of the PMSG. The PMSG and the full-scale converter have an increasing market share in variable speed Wind Energy Conversion System (WECS). When compared to the Induction Generators (IGs), the PMSGs are smaller, easier to control and more efficient. In addition, the PMSG can operate at variable speeds, so that the maximum power can be extracted even at low or medium wind speeds. Wind turbines generally employ speed sensors or shaft position encoders to determine the speed and the position of the rotor. In order to reduce the cost, maintenance and complexity concerned with the sensor, the sensor-less approach has been developed. This study presents the sensor-less control techniques using the flux-linkage and the back EMF estimation methods. Simulations for both the methods are carried out in MATLAB/SIMULINK. The simulated waveforms of the reference speed, the measured speed, the reference torque, the measured torque and rotor position are shown for both the methods.

Keywords: Back EMF estimation method, Field Oriented Control (FOC), flux linkage estimation method, Permanent Magnet Synchronous Generator (PMSG), sensor-less control

INTRODUCTION

Variable-speed wind generation with the PMSG and a full-scale power electronic converter is a promising but not yet a very popular wind turbine concept. A PMSG connected to a power electronic converter can operate at low speeds, so a gearbox is not required. Since the gearbox increases the weight, the losses, the costs and demands more maintenance, a gearless construction represents an efficient and a robust solution, especially for offshore applications. Also, due to the presence of the permanent magnet in the PMSG, the DC excitation system can be eliminated, further reducing the weight, the losses, the costs and the maintenance requirements (Hsieh and Hsu, 2012; Qiao *et al*., 2012). Thus, the efficiency of a PMSG based wind energy system is higher than other variable-speed WECS. In addition, a full-scale Insulated-Gate Bipolar Transistor (IGBT) converter allows full controllability of the system (Li *et al*., 2009, 2010). The generator-side converter controls the generator speed to enhance the wind power extraction. The control techniques for the generator-side converter decouple the torque and flux controls. Vector control or direct control technique is used for this purpose. A rotor field oriented control is applied to the generator-side converter to control the generator speed and to obtain the maximum electromagnetic torque with the minimum current. To achieve this, the d-component of the stator currents is forced to zero and the electromagnetic torque is controlled only with the q-component of the current. When compared to the direct control, vector control achieves higher overall system efficiency, which is mainly due to the lower current distortion and the consequent lower joule losses (Freire *et al*., 2012).

Several techniques are available for the sensor-less position and speed estimations. In Fan *et al*. (2010), a digital phase-locked loop is used for the sensor-less vector control of speed and position. This controls the frequency of the output signal by a control signal that is proportional to the difference between the output phase of the system and the phase of the given signal. With this obtained frequency characteristic, the motor speed and the rotor position angle are measured. However, this frequency control technique does not work well when the motor runs at low speed. In Zhonggang *et al*. (2012), a Robust Extended Kalman Filter (REKF) algorithm is used for the sensor-less vector control. Although this method provides less effect of gross error on the estimation accuracy, the intensive calculations involved are difficult to compute and time consuming.

Corresponding Author: Porselvi Thayumanavan, Department of EEE, Sri SaiRam Engineering College, Chennai, India

High frequency signals injection method (Consoli *et al*., 2001) is proven effective at low-speeds and even at standstill for both the salient and non-salient pole machines. However, the method requires additional carrier signals, resulting in unnecessary losses, current and torque distortions and acoustic noise.

A speed controller observer based on the model reference adaptive control was proposed for the Permanent Magnet Synchronous Motor (PMSM) in Saikumar and Sivakumar (2011), Maiti *et al*. (2008) and Kim *et al*. (1995). This controller requires two models, which increase the complexity in the control and the costs. In Yongchang *et al*. (2009), a comparison between a Luenberger observer, a sliding mode observer and an extended Kalman filter was made for the sensor-less control of the induction machine. It was shown that the first two methods are more suitable when compared to the third method.

This study describes the sensor-less vector control method of the PMSG. There are several methods of sensor-less control of PMSG available. Two methods are considered namely the flux linkage estimation method and the back EMF estimation method. Simulation is carried out in MATLAB/SIMULINK for both the methods. A comparison based on the settling time of speed and torque for the two methods is shown. The simulated waveforms of the stator voltage, the stator current, the reference speed, the measured speed, the reference torque, the measured torque and the rotor position are shown for both the methods for varying reference speed and reference torque.

MATERIALS AND METHODS

Modeling of the PMSG: Equation (1) gives the mathematical model of the PMSG derived from the stator voltage equation:

$$v_S = R_S i_S + \frac{d}{dt}\Psi_S \tag{1}$$

where, v_s, i_s and Ψ_s are the space vectors of the stator voltages, the stator currents and the flux linkages, respectively.

Equation (2) and (3) give the voltage equations in the d-q reference frame with the d-axis coinciding with the permanent magnet pole axis:

$$v_{sd} = R_S i_{sd} + \frac{d\Psi_d}{dt} - \omega_e \Psi_q \tag{2}$$

$$v_{sq} = R_S i_{sq} + \frac{d\Psi_q}{dt} + \omega_e \Psi_d \tag{3}$$

where, ω_e is the electrical speed in rad/s.

Equation (4) and (5) give the flux linkages in the d-q reference frame:

$$\Psi_d = L_d i_{sd} + \Psi_m \tag{4}$$

$$\Psi_q = L_q i_{sq} \tag{5}$$

where, ψ_d and ψ_q are the d-axis and q-axis flux linkages, respectively, L_d and L_q are the d-axis and the q-axis inductances, respectively and ψ_m is the permanent magnet flux linkage.

Equation (6) gives the electromagnetic power from which the electromagnetic torque derived:

$$P_{em} = \frac{3}{2}\omega_e(\Psi_d i_{sq} - \Psi_q i_{sd}) \tag{6}$$

Equation (7) gives the relation between the electrical and the mechanical speed:

$$\omega_e = p\,\omega_m \tag{7}$$

where,
p = The number of pole pairs
ω_m = The mechanical speed of the rotor

Hence, Eq. (8) gives the expression for the electromagnetic torque:

$$T_e = \frac{P_{em}}{\omega_m} = \frac{3}{2}p(\Psi_d i_{sq} - \Psi_q i_{sd}) \tag{8}$$

By substituting the d-axis and the q-axis flux linkages in Eq. (8) and by considering that the d-axis and q-axis inductances for the surface mounted PMSG are equal, the torque relation is finally derived and given by Eq. (9):

$$T_e = \frac{3}{2}p(\Psi_m i_{sq}) \tag{9}$$

Equation (10) shows the general mechanical equation of the machine:

$$T_e = T_L + B\omega_m + T_d + J\frac{d}{dt}\omega_m \tag{10}$$

where,
T_L = The load torque
J = The moment of inertia
B = The viscous frictional coefficient

Field oriented control: Field Oriented Control (FOC) is a vector control technique, which controls the torque indirectly by controlling the stator currents. The constant torque angle control is used in this study. In this method, the torque angle is kept at 90°. The d-axis current component is set to zero and therefore the stator current has only the q-axis component. Since the torque angle and the permanent magnet flux are

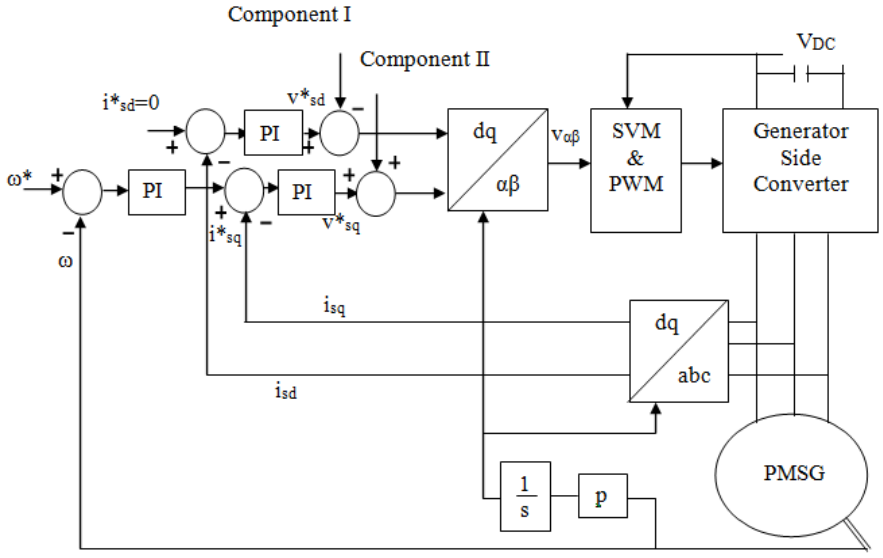

Fig. 1: Field oriented control of the PMSG with the sensor

constant, the torque depends only on the q-axis stator current.

As the current control is performed on the rotor reference frame, a transformation of coordinates is required to obtain the reference stator currents. FOC eliminates current cross coupling between the d and q axes components, which requires feed-forward compensation. In the FOC, the permanent magnet flux linkage is aligned along the d-axis.

Figure 1 gives the block diagram of the FOC of the PMSG with the sensor. In this control, the speed is sensed and compared with the reference speed. The error in speed is processed in the PI controller to obtain the reference q-axis current. The reference d-axis current is set to zero. The stator currents from the PMSG are transformed to the d-q reference frame and compared with the reference d-q currents.

For decoupling purposes, a feed-forward loop is used. This includes the components I and II, which are given by:

Component I: $\omega_e \Psi_q = \omega_e i_{sq} L_q$

Component II: $\omega_e \Psi_d = \omega_e i_{sd} L_d + \Psi_m$

V_{dc} and $V_{\alpha\beta}$ are given to space vector modulation block to produce the gate signals for the converter switches.

q-axis current controller design: Figure 2 shows the block diagram for the design of the q-axis current controller. The various blocks are the PI block, the delay introduced by the PI, the delay introduced by the inverter, the plant that is the stator block and the delay

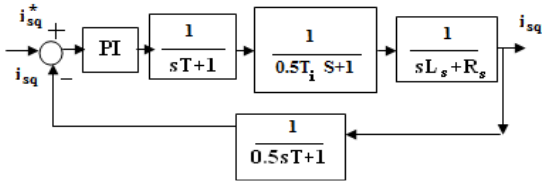

Fig. 2: Block diagram for the design of the q-axis current controller

introduced due the digital to analog conversion, which is taken to be equal to half of the delay introduced by the PI.

Equation (11) gives the transfer function of the q-axis current controller:

$$G_q(s) = K_{pq}\left(1+\frac{1}{sT_{iq}}\right) \quad (11)$$

where,

K_{pq} = The proportional gain of the q-axis current controller

T_{iq} = The integral time constant of the q-axis current controller

d-axis current controller design: The d-axis current controller is implemented in the same way as the q-axis current controller except that the L_q is replaced by L_d. Equation (12) gives the transfer function of the d-axis current controller:

$$G_d(s) = K_{pd}\left(1+\frac{1}{sT_{id}}\right) \quad (12)$$

where,

K_{pd} = The proportional gain of the d-axis current controller

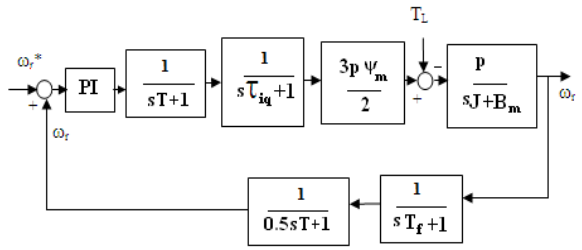

Fig. 3: Design of the speed controller

T_{id} = The integral time constant of the d-axis current controller

q-axis speed controller design: Figure 3 shows the block diagram for the design of the speed controller, where, $\tau_{iq} = L_q/R_s$, p is the number of pole pairs, T_f is the filter time constant used only when an encoder measures the speed.

Equation (13) gives the transfer function of the PI speed controller:

$$G_\omega(s) = K_{p\omega}\left(1+\frac{1}{sT_{i\omega}}\right) \quad (13)$$

where,
$K_{p\omega}$ = The proportional gain of the speed controller
$T_{i\omega}$ = The integral time constant of the speed controller

Sensor-less control: Using a sensor to encode the speed has several drawbacks like, increased cost, bigger size and lower reliability of the system. This study, therefore, presents the sensor-less control methods using the flux linkage and the back-EMF estimation methods.

Figure 4 shows the block diagram of the FOC of the PMSG without the sensor. In this control, the stator currents from the PMSG are taken and transformed to the α-β reference frame. The currents in the α-β reference frame are given to the position and speed estimation blocks.

Flux linkage estimation method: This method is used for estimating the position of the rotor. The rotor position estimation is based on the estimation of the flux linkages. The initial rotor position is found from the flux linkage using the inductances and the stator currents (Lukko, 2000). Sensor-less control method is implemented in five steps:

Step 1: Estimation of the stator flux linkages: Phase currents and voltages are assumed to be measured at a fixed sample time T_s. The stator flux linkages are given in Eq. (14) and (15):

$$\Psi_\alpha(k) = T_S[v(k-1) - R_S i_\alpha(k)] + \Psi_\alpha(k-1) \quad (14)$$

$$\Psi_\beta(k) = T_S[v(k-1) - R_S i_\beta(k)] + \Psi_\beta(k-1) \quad (15)$$

where, k is the present sampling interval and k-1 is the previous sampling interval. The currents i_α and i_β (i.e., the stator currents in the stationary reference frame) are obtained by measuring the a, the b and the c stator phase currents.

Step 2: Stator current estimation: The stator currents are estimated by the flux linkages estimated in step 1 and the predicted rotor position in step 5. The stator currents are then estimated using Eq. (16) and (17):

$$\Psi_\alpha = -\Delta L \sin(2\theta_r) i_\beta + (L - \Delta L\cos(2\theta_r)) i_\alpha + \Psi_m \cos\theta_r \quad (16)$$

$$\Psi_\beta = -\Delta L \sin(2\theta_r) i_\alpha + (L + \Delta L\cos(2\theta_r)) i_\beta + \Psi_m \sin\theta_r \quad (17)$$

where, $L = \frac{L_d + L_q}{2}$ and $\Delta L = \frac{L_q - L_d}{2}$.

Figure 5 shows the various steps involved in the estimation of rotor position.

Step 3: Position correction: In this step, the rotor position predicted in step 5 is corrected with the errors of the stator currents. The errors of the current are obtained from the difference between the measured and estimated currents. Equation (18) and (19) give the errors of the current in the d and q axes reference frames, respectively:

$$\Delta i_q = \Delta i_\beta \cos(\theta_p) - \Delta i_\alpha \sin(\theta_p) \quad (18)$$

$$\Delta i_d = \Delta i_\beta \sin(\theta_p) + \Delta i_\alpha \cos(\theta_p) \quad (19)$$

The corrected position is obtained by adding the position error to the predicted position, as given in Eq. (20):

$$\theta_r(k) = \theta_p(k) + \Delta\theta(k) \quad (20)$$

where, Θ_r and Θ_p are the corrected and the predicted rotor angles respectively.

Step 4: Flux linkage updating: In this step, the fluxes are recalculated using the corrected rotor position and the measured stator currents. Equation (21) and (22) express the fluxes in discrete time:

$$\Psi_\alpha(k) = [L - \Delta L\cos(2\theta_r(k))] i_\alpha(k) - \Delta L \sin(2\theta_r(k)) i_\beta(k) + \Psi_m \cos(\theta_r(k)) \quad (21)$$

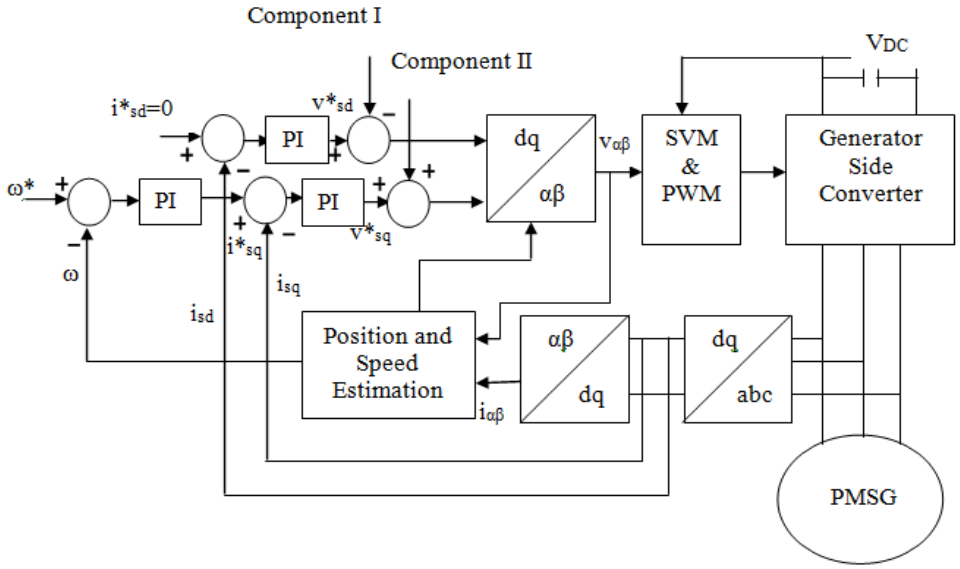

Fig. 4: Field oriented control of the PMSG without the sensor

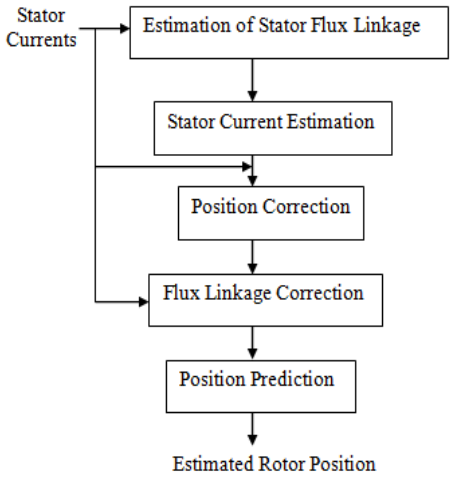

Fig. 5: Steps for the estimation of rotor position

$$\Psi_\beta(k) = [L + \Delta L\cos(2\theta_r(k))]i_\beta(k) - \Delta L\sin(2\theta_r(k))i_\alpha(k) + \Psi_m \sin(\theta_r(k)) \quad (22)$$

Step 5: Position prediction: Considering position to be a second-order polynomial, the position prediction can be expressed by Eq. (23):

$$\theta_p = et^2 + ft + g \quad (23)$$

where, e, f, g are constants (Chandana Perera, 2002).

Back-EMF estimation method: The permanent magnet flux is aligned with the d-axis, while the induced voltage of the permanent magnet flux i.e., the back-EMF is along the q-axis. This back EMF can be used to calculate the rotor position. The rotor is in the same position as that of the back EMF, as shown in Fig. 6.

The position of the back EMF space vector is determined using Eq. (24):

$$\theta_r = \tan^{-1}\frac{e^s d}{e^s q} \quad (24)$$

In order to have a simpler model, the Clarke's transformation is used. Equation (25) gives the relation between the abc and the α-β reference frames:

$$\begin{bmatrix} v\alpha \\ v\beta \end{bmatrix} = \frac{2}{3}\begin{bmatrix} 1 & -\frac{1}{2} & -\frac{1}{2} \\ 0 & \frac{\sqrt{3}}{2} & -\frac{\sqrt{3}}{2} \end{bmatrix}\begin{bmatrix} v_a \\ v_b \\ v_c \end{bmatrix} \quad (25)$$

By knowing the voltages of the stator in the α-ß reference frame, the stator angle is calculated as by Eq. (26):

$$\theta_v = \tan^{-1}\frac{v_\beta}{v_\alpha} \quad (26)$$

where, v_α and v_β are the stator voltages in the α-ß reference frame.

Now, the variables in the α-β reference frame are transformed into a new reference frame of δ-φ, which is shown in Fig. 7.

Equation (27) gives the transformation matrix that converts the α-β variables to the δ-φ variables:

$$\begin{bmatrix} v_\delta \\ v_\varphi \end{bmatrix} = \begin{bmatrix} \cos\theta_v & \sin\theta_v \\ -\sin\theta_v & \cos\theta_v \end{bmatrix}\begin{bmatrix} v_\alpha \\ v_\beta \end{bmatrix} \quad (27)$$

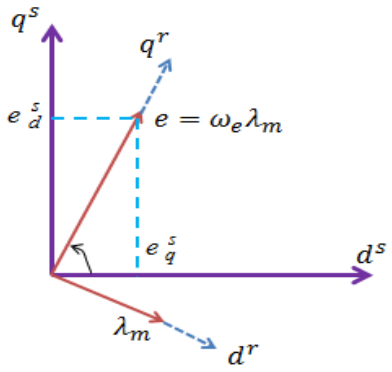

Fig. 6: Space vector representation of the back EMF

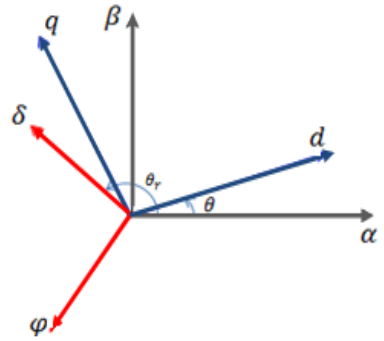

Fig. 7: Relationship between α-β and δ-φ frame

Now, the stator voltage is aligned with the δ axis with the v_φ component equal to zero. The voltage equations of the PMSG in the δ-φ co-ordinate system are given by Eq. (28) and (29):

$$v_\delta = R_s i_\delta + L_s \frac{di_\delta}{dt} - \omega_i L_s i_\delta + e_\delta \quad (28)$$

$$v_\phi = R_s i_\varphi + L_s \frac{di_\varphi}{dt} + \omega_i L_s i_\varphi + e_\varphi \quad (29)$$

where,
ω_i = The rotational speed of i_s
e_δ and e_φ = Back EMFS of the stator in δ-φ reference frame, respectively

They can be expressed by Eq. (30) and (31):

$$e_\delta = \omega_e \lambda_m \sin\theta_n \quad (30)$$

$$e_\varphi = \omega_e \lambda_m \cos\theta_n \quad (31)$$

where,
ω_e = The rotor electrical speed
λ_m = The permanent magnet flux linkage
Θ_n = The estimated rotor angle in δ-φ reference frame

At steady state, the currents i_δ and i_φ are constant, resulting in the derivative term of the Eq. (28) and (29) becoming zero. Assuming ideal conditions, the rotor position in the δ-φ reference frame is determined from Eq. (30) and (31) and is expressed by Eq. (32):

$$\theta_n = \tan^{-1} \frac{v_\delta - R_s i_\delta + \omega_i L_s i_\delta}{v_\varphi - R_s i_\delta - \omega_i L_s i_\varphi} \quad (32)$$

Equation (33) gives the estimated rotor position:

$$\theta = \theta_v - \theta_n \quad (33)$$

RESULTS AND DISCUSSION

The system is simulated in MATLAB/SIMULINK for the sensor-less field oriented control with the flux linkage and back-EMF estimation methods. The initial reference speed and torque are 700 rpm and -9 Nm, respectively. Then the reference speed alone is changed to 1000 rpm at 2 sec with the same torque. At 4 sec, the reference torque is changed to -12 Nm, with the speed reference at 1000 rpm. Figure 8 and 9, respectively

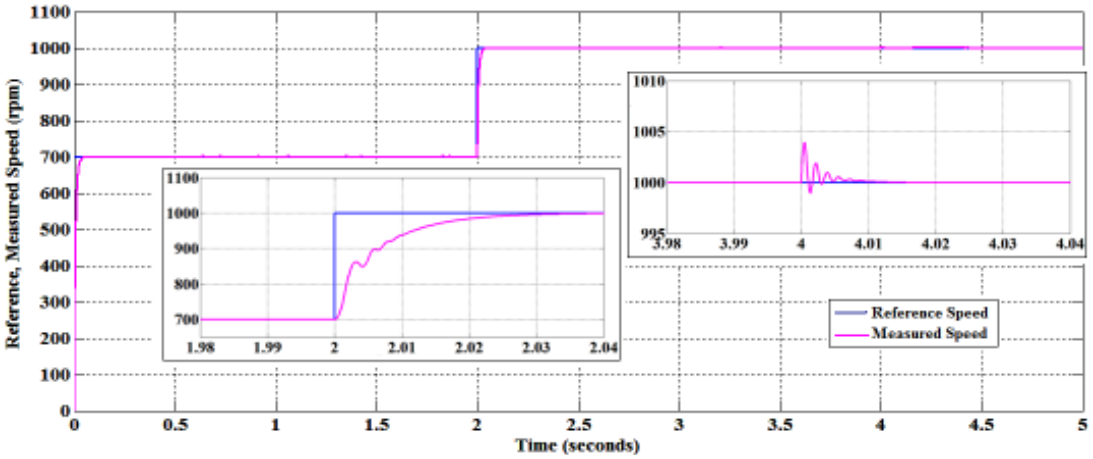

Fig. 8: The reference and measured speeds of the PMSG for the flux linkage estimation method

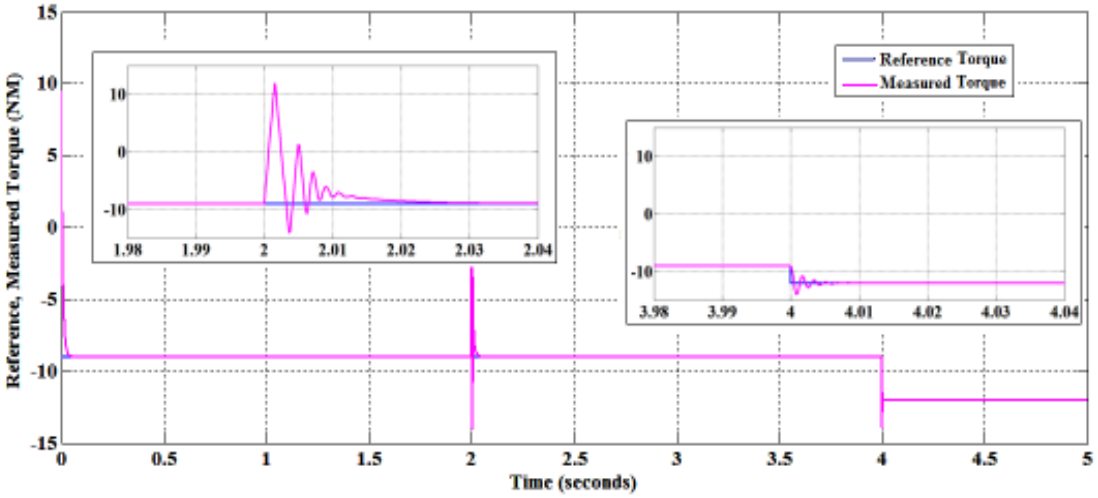

Fig. 9: The reference and measured torques of the PMSG for the flux linkage estimation method

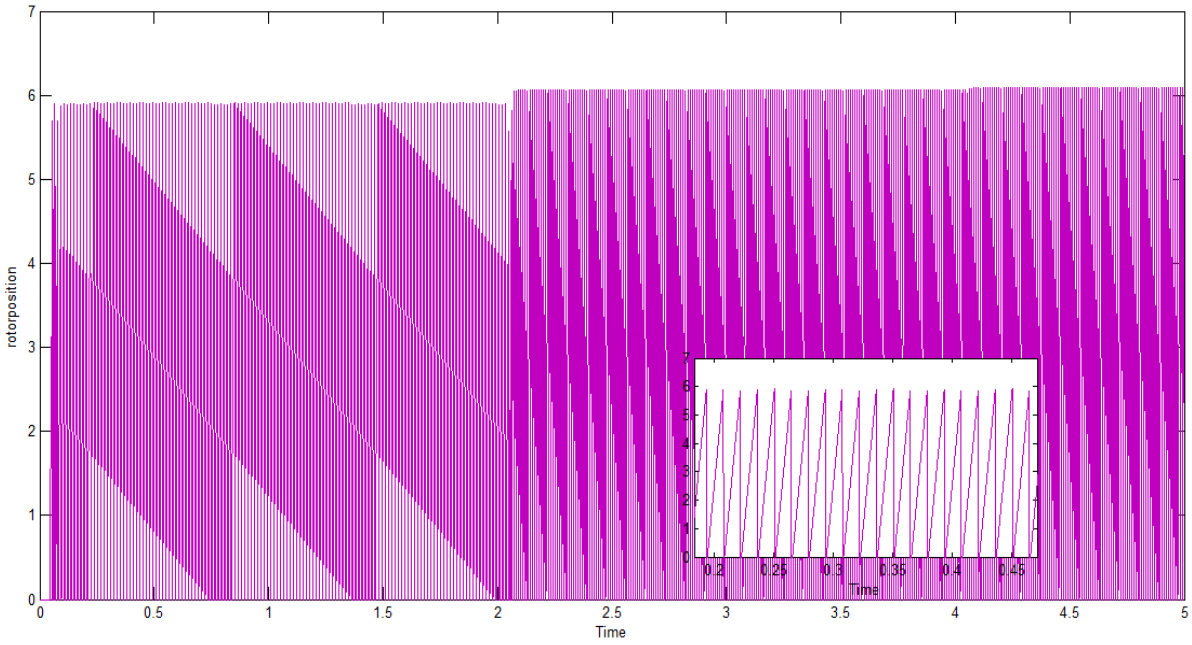

Fig. 10: Measured and estimated rotor positions for the flux linkage estimation method

show the reference and measured speeds and the reference and measured torques for the flux linkage estimation method. Figure 10 shows the measured and estimated rotor position for the flux linkage estimation method.

Figure 11 and 12, respectively show the reference and measured speeds and the reference and measured torques for the back-EMF estimation method.

From the Fig. 8 and 11, it is found that the speed follows the reference speed. Initially, when the reference speed was set at 700 rpm, the PMSG follows the reference speed of 700 rpm. When the reference speed changes to 1000 rpm at t = 2 sec, the speed of the PMSG also changes and reaches the reference speed within 0.028 sec for the flux linkage and the back-EMF methods. There is a little oscillation in speed at t = 4 sec which is due to the change in the reference torque, which also damps out within 0.01 sec for the flux linkage method. However, some oscillations exist in back-EMF estimation method, which damps out within 0.015 sec. It is found from the Fig. 11 that, there are some oscillations speed in the system with the change in the reference speed and torque for the back EMF estimation method.

From Fig. 9 and 12, it is found that the torque follows the reference torque of -9 Nm up to t = 4 sec. The torque oscillates at 2 sec due to the change in the reference speed. The oscillation is damped out in 0.02 sec for the flux linkage method and in 0.025 sec for the back EMF method. When the torque reference is

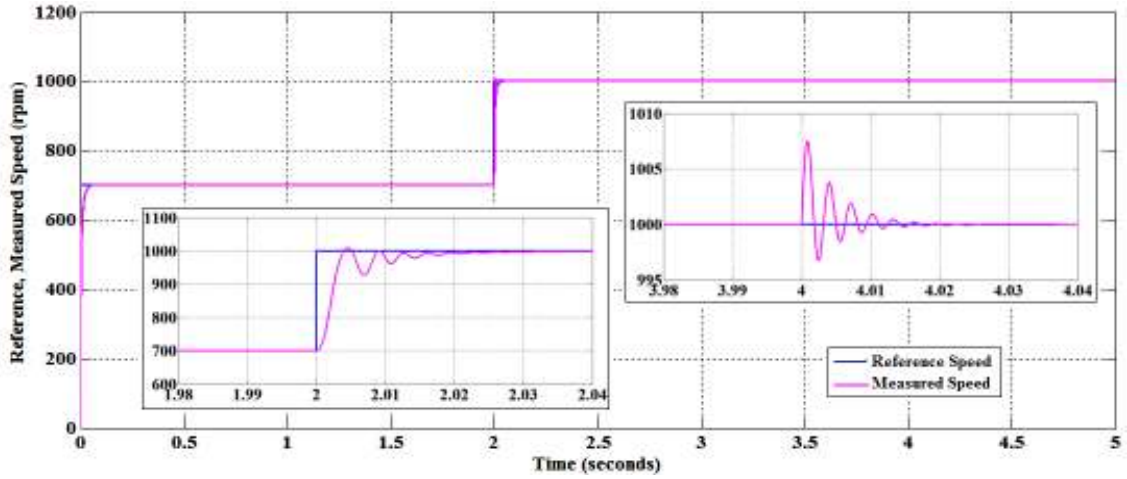

Fig. 11: Reference and measured speeds of the PMSG for the back-EMF estimation method

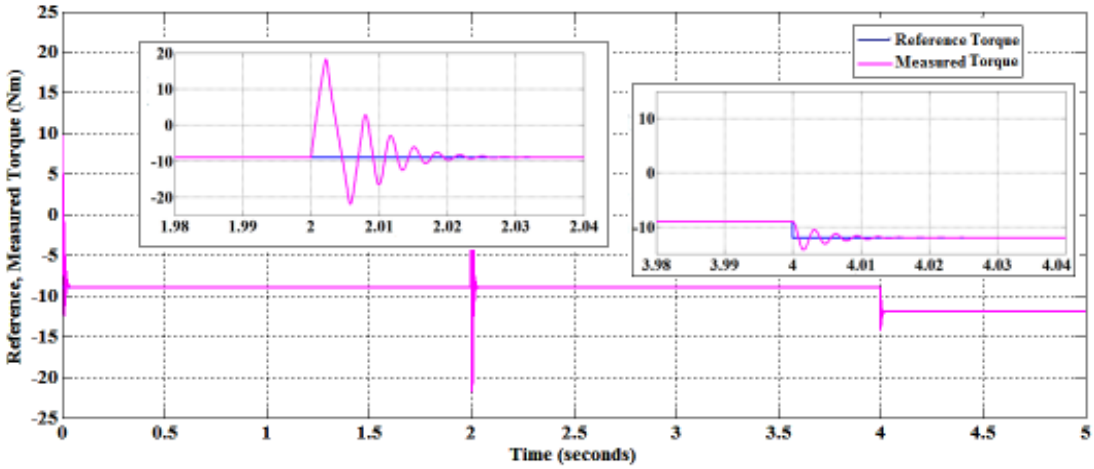

Fig. 12: Reference and measured torque of PMSG for the back EMF estimation method

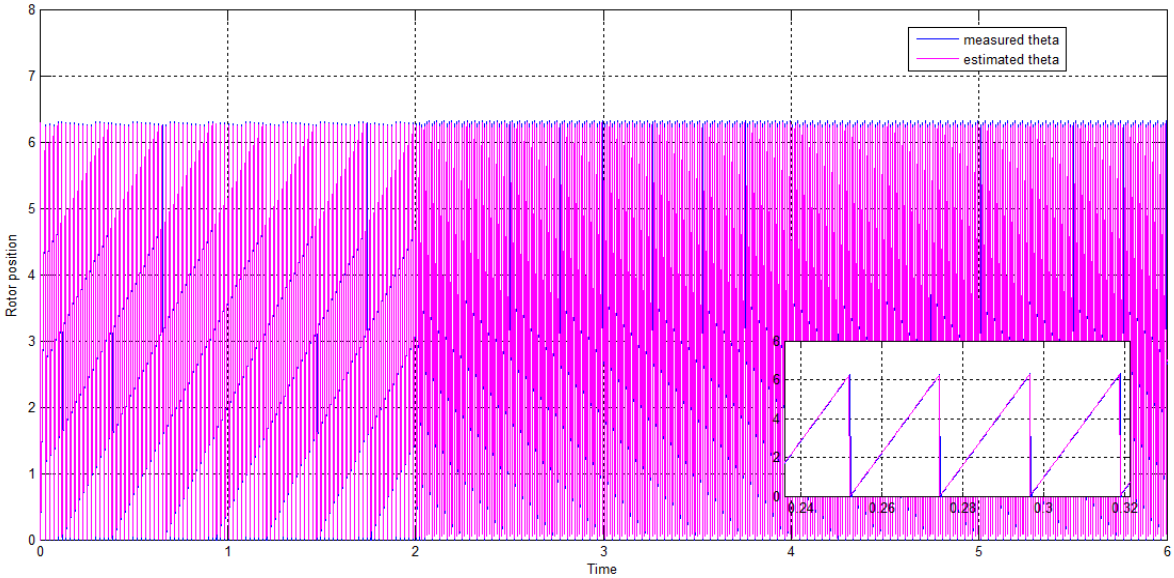

Fig. 13: The measured and the estimated rotor position for the back-EMF estimation method

Table 1: Comparison of the flux linkage and back EMF methods

	Settling time for speed (sec)		Settling time for torque (sec)	
Method	Due to change in speed reference	Due to change in torque reference	Due to change in speed reference	Due to change in torque reference
Flux linkage estimation method	0.028	0.010	0.020	0.005
Back EMF estimation method	0.028	0.015	0.025	0.010

changed to -12 Nm at t = 4 sec, it is seen that the torque of the PMSG also changes and reaches the reference torque within 0.005 sec for the flux linkage method and within 0.01 sec for the back-EMF method.

Figure 13 shows the measured and estimated rotor positions for the back-EMF estimation method.

Table 1 shows the comparison of the flux linkage and the back EMF estimation methods based on the settling time of speed and torque for change in speed and torque.

It is found from the Fig. 8, 9, 11 and 12 and the Table 1, that the response for the flux linkage method is faster than the back-EMF method. In addition, it is evident from the waveforms that, the presence of oscillations is more in the back-EMF method.

CONCLUSION

The PMSG is modelled in the d-q reference frame with the d-axis aligned with the permanent magnet axis. The PMSG is controlled with a sensor-less field oriented control for varying reference speeds and torques. The sensor-less tracking of the position and the speed of the PMSG is carried out using the flux linkage estimation method and the back-EMF estimation methods. The two control methods are simulated using the MATLAB/SIMULINK. The flux linkage estimation method shows a faster response to the change in reference speed and torque. This improves the robustness and the effectiveness of the system. In spite of the many advantages, this algorithm uses sampled data from the previous time instant, which introduces certain time delay in the system and presents integration drift problems. The back-EMF method presents certain oscillations in the system with the change in the reference speed and torque and has sensitivity problems with parameter changes. The main drawback of the back-EMF estimation method is the estimation of the position of the rotor at zero speed or low speed ranges, because the back EMF becomes zero and thus the position estimation is not possible. At low speeds, the back-EMF is very small which leads to a large error in the estimation. From the simulated results, it is observed that better control is achieved with the flux linkage estimation method as compared to the back-EMF estimation method.

REFERENCES

Chandana Perera, P.D., 2002. Sensorless control of permanent magnet synchronous motor drives. M.A. Thesis, Institute of Energy Technology, Aalborg University, Denmark.

Consoli, B., G. Scarcella and A. Testa, 2001. Industry application of zero-speed sensorless control techniques for PMSM. IEEE T. Ind. Appl., 37: 513-521.

Fan, S., P. Wang and C. Wen, 2010. A new sensorless control strategy used in direct-drive PMSG wind power system. Proceeding of the 2nd IEEE International Symposium on Power Electronics for Distributed Generation Systems. Hefei, China, pp: 611-615.

Freire, N., J. Estima and A.J.M. Cardoso, 2012. A comparative analysis of PMSG drives based on vector control and direct control technique for wind turbine applications. Prz. Elektrotechniczn., 88(1a): 184-187.

Hsieh, M.F. and Y.C. Hsu, 2012. A generalized magnetic circuit modeling approach for design of surface permanent-magnet machines. IEEE T. Ind. Electron., 50: 779-792.

Kim, K.M., S.K. Chung, G.W. Moon, I.C. Baik, M. Jy and M. Youn, 1995. Parameter estimation and control for permanent magnet synchronous motor drive using model reference adaptive technique. Proceedings of the 21st International Conference on Industrial Electronics, Control and Instrumentation (IEEE-IECON). Orlando, FL, 1: 387-392.

Li, S., T.A. Haskew and L. Xu, 2010. Conventional and novel control designs for direct driven PMSG wind turbines. Electr. Pow. Syst. Res., 80: 328-338.

Li, S., T.A. Haskew, E. Muliadi and C. Serrentino, 2009. Characteristic study of vector-controlled direct-driven permanent magnet synchronous generator in wind power generation. Electr. Pow. Compo. Sys., 37(10): 1162-1179.

Lukko, J., 2000. Direct torque control of permanent magnet synchronous machines-analysis and implementation. Ph.D. Thesis, Acta. Universitatis Lappeenrantaensis.

Maiti, S., C. Chakraborty, Y. Hori and M.C. Ta, 2008. Model reference adaptive controller-based rotor resistance and speed estimation techniques for Vector controlled induction motor drive utilizing reactive power. IEEE T. Ind. Electron., 55: 594-601.

Qiao, W., X. Yang and X. Gong, 2012. Wind speed and rotor position sensorless control for direct-drive PMG wind turbines. IEEE T. Ind. Appl., 48: 3-11.

Saikumar, P. and J.S.V. Sivakumar, 2011. Model reference adaptive controlled application to the vector controlled permanent magnet synchronous motor drive. Int. J. Power Energ., 1: 35-41.

Yongchang, Z., Z. Zhengming, L. Ting, Y. Liqiang, X. Wei and Z. Jianguo, 2009. A comparative study of Luenberger observer, sliding mode observer and Kalman filter for sensorless vector control of induction motor drives. Proceeding of the IEEE Energy Conversion Congress and Exposition (ECCE-2009). San Jose, CA, pp: 2466-2473.

Zhonggang, Y., Z. Ruifeng, Z. Yanru and C. Yu, 2012. Speed and Flux estimation of permanent magnet synchronous motor for sensorless vector control based on robust extended Kalman filter. Proceeding of the IEEE International Symposium on Industrial Electronics. Hangzhou, pp: 748-751.